

Improving transparency of stretched PET/MXD6 blends by modifying PET with isophthalate

Y.S. Hu^a, V. Prattipati^a, A. Hiltner^{a,*}, E. Baer^a, S. Mehta^b

^aDepartment of Macromolecular Science, Center for Applied Polymer Research, Case Western Reserve University, Kent Hale Smith Building, Room 423, 10900 Euclid Ave., Cleveland, OH 44106-7202, USA

^bINVISTA, 1551 Sha Lane, Spartanburg, SC 29304, USA

Received 28 February 2005; received in revised form 10 April 2005; accepted 11 April 2005

Available online 5 May 2005

Abstract

Compatibilized blends of PET and MXD6 have good transparency because their refractive indices match closely. However, haziness is observed when the blends are stretched because stretching imparts greater refractive index anisotropy to PET than to MXD6. Analysis of the strain-dependent birefringence reveals that different molecular deformation models describe the intrinsic birefringence of PET and MXD6. This study focuses on reducing the intrinsic birefringence of PET by partially replacing terephthalate with isophthalate. Statistical copolymers are prepared by conventional copolymerization of the monomers. Alternatively, blocky copolymers are obtained by melt blending PET with poly(ethylene isophthalate) (PEI). A close refractive index match with stretched MXD6 is achieved with copolymers containing 15–20% isophthalate. Statistical copolymers in this composition range are not satisfactory for blending because they have low molecular weight and are difficult to stretch. However, blocky copolymers containing 15–20% isophthalate form blends that stretch readily. After biaxial stretching, transparency of blends with 10 wt% MXD6 approaches that of PET. Good transparency of the blends is validated with stretch-blown bottle walls. Oxygen transport measurements confirm that partial replacement of terephthalate with isophthalate does not affect the good gas barrier properties of biaxially stretched PET blends.

© 2005 Elsevier Ltd. All rights reserved.

Keywords: PET blends; Birefringence; Transparency

1. Introduction

The oxygen permeability of poly(ethylene terephthalate) (PET) can be dramatically reduced by blending with a high barrier aromatic polyamide [1]. Biaxial orientation, such as imparted by the stretch-blow molding process, transforms spherical polyamide particles into platelets of high aspect ratio arrayed in the plane of the film [2]. Reduction in oxygen permeability by as much as a factor of 3 with 10 wt% polyamide is due to increased tortuosity of the diffusion pathway.

Good refractive index match between PET and poly(*m*-xylylene adipamide) (MXD6) results in blends that are almost as transparent as PET. However, haziness has been

observed in biaxially oriented films [3,4], and in stretch-blown bottles [5]. Two contributing factors have been identified [6], particle size and refractive index mismatch. Incompatibility of PET and MXD6 results in large MXD6 particles that can effectively scatter light. Compatibilization with a functionalized PET copolymer reduces particle size to the submicron level [1,2]. However, biaxial stretching transforms small spherical particles into large-diameter platelets that can produce haziness if there is a mismatch in the refractive indices. In order to reduce the dimension of the platelets below the quarter wavelength, it is estimated that the particle size in unstretched blends must be smaller than 50 nm [7]. This result can not be achieved by increasing the amount of compatibilizer alone [7]. An alternative strategy for achieving transparency depends on matching refractive indices of the blend constituents.

It was demonstrated that the good transparency of glassy PET blends with MXD6 was lost after orientation because stretching imparts greater refractive index anisotropy to PET than to MXD6 [7]. Hence, to achieve better

* Corresponding author.

E-mail address: pah6@cwru.edu (A. Hiltner).

transparency in the oriented blend, refractive index matching needs to focus on the oriented constituents. One approach is to increase the refractive index of the polyamide. In a previous study [7], adipamide in MXD6 was partially replaced with isophthalamide by copolymerization. Although this approach succeeded in increasing the refractive index of the polyamide, disappointingly low transparency of the resulting oriented blends with PET was attributed to poor orientation of the copolyamide particles as a result of their increased glass transition temperature.

A second approach focuses on reducing the intrinsic birefringence of the PET matrix by partial replacement of terephthalate with meta-substituted isophthalate. This substitution should disrupt alignment of the PET chains and thereby reduce the refractive index anisotropy. One method for incorporating isophthalate is conventional copolymerization of the monomers. Unfortunately, statistical copolymers with more than 10% isophthalate may not be satisfactory matrix polymers for blends with polyamides because they have low molecular weight and reportedly are difficult to stretch [8]. Alternatively, when PET is melt blended with poly(ethylene isophthalate) (PEI), relatively little transesterification occurs during melt blending, as demonstrated previously by ^{13}C NMR [8]. Accordingly, melt blends closely resemble block copolymers. Such blocky copolymers containing up to 30% isophthalate maintain high molecular weight and are reported to stretch readily [8]. In the present study, isophthalate is incorporated into PET both by conventional copolymerization to produce statistical copolymers and by melt blending of the homopolymers to create blocky copolymers. The effect of stretching on refractive index and transparency of the copolymers and their blends with MXD6 is examined.

2. Materials and methods

Poly(ethylene terephthalate) (PET), poly(ethylene isophthalate) (PEI) and statistical copolymers with 7, 20 and 30% isophthalate (PET-*co*-7I, PET-*co*-20I and PET-*co*-30I) were provided by INVISTA (Spartanburg, SC, USA) in the form of extruded pellets. A copolymer with 2.29 mol% terephthalate in PET replaced with sodium 5-sulfoisophthalate (PET-*co*-SIPE) was also provided in the form of extruded pellets as a compatibilizer for blends with MXD6. The copolymers were polymerized according to the methodology described previously [9]. The intrinsic viscosity was measured at 25 °C in dichloroacetic acid solution. Poly(*m*-xylylene adipamide) (MXD6) with $M_n = 16,500$ was obtained from Mitsubishi Gas Chemical America, Inc., in pellet form.

For melt blending, PET and PEI pellets were dried at 80 and 50 °C, respectively, for 48 h in vacuo and dry blended to give compositions with 15, 20, 25 and 30% PEI (PET-*b*-15I, PET-*b*-20I, PET-*b*-25I and PET-*b*-30I). The dry blends were extruded in a DACA twin-screw extruder with

partially co-rotating and self-wiping conical screws. The screws had diameter of 13.75 mm and length of 108 mm. The barrel temperature was 270 °C and the screw speed was 100 rpm. The residence time was approximately 2 min for each 4 g batch. The molten blends were extruded through a 2 mm die and pelletized.

Before melt blending the polyesters with MXD6, the polymers were dried for 48 h in vacuo. The drying temperature was 80 °C for PET, PET-*co*-7I, all the blocky copolymers, PET-*co*-SIPE and MXD6 pellets, and was 60 °C for PET-*co*-20I and PET-*co*-30I pellets. The polyester constituents were dry blended with 10 wt% MXD6 and extruded in the DACA twin screw extruder. The PET control was similarly dried and extruded. During melt blending, miscibility and transesterification of PET-*co*-SIPE with the other matrix polyester constituent produced a homogeneous polyester matrix with 0.38 mol% sodium 5-sulfoisophthalate.

Extruded controls and blends were dried in vacuo at 80 °C for 48 h before molding into films, except for PET-*co*-20I and PET-*co*-30I which were dried at 60 °C. The dried pellets were compression-molded between Kapton films and quenched into ice water as described previously [10]. The platens were heated in the press at 270 °C for 4 min with repeated application and release of pressure to remove air bubbles, and held at 309 ψ (2.1 MPa) for an additional 4 min. Films of approximately 0.20, 0.40 and 0.60 mm thickness were prepared in this manner.

Films of PET and the blends were dried at 70 °C and MXD6 was dried at 80 °C for 2 days to obtain thermograms of the dry materials. Thermal analysis was conducted with a Perkin-Elmer Pyris-1 calibrated with indium and tin. The heating scans were performed at 10 °C min^{-1} from 30 to 270 °C.

Blend morphology was examined with atomic force microscopy (AFM) using the Nanoscope IIIa MultiMode head from Digital Instruments (Santa Barbara, CA, USA) in the tapping mode. Specimens were microtomed at ambient temperature to expose the bulk morphology. Phase and height images were recorded simultaneously.

Compression-molded films were conditioned at 43% relative humidity (RH), which decreased the T_g and facilitated orientation of the MXD6 domains. After conditioning to equilibrium, the films were uniaxially and sequentially biaxially stretched in the environmental chamber of an Instron mechanical testing machine at a strain rate of 20% min^{-1} . For constrained uniaxial orientation, compression-molded films 150 mm wide, 40 mm long and 0.40 mm thick were stretched at 75 °C to a target draw ratio of 4. For sequential biaxial orientation, compression-molded films 150 mm wide, 40 mm long and 0.60 mm thick were stretched uniaxially at 75 °C to a target draw ratio of 4, remounted in the grips at 90° to the first stretch direction and stretched again at 78 °C to achieve a target balanced biaxial draw ratio of 2.7 \times 2.7. Grids were marked on the specimens for measuring the draw ratio.

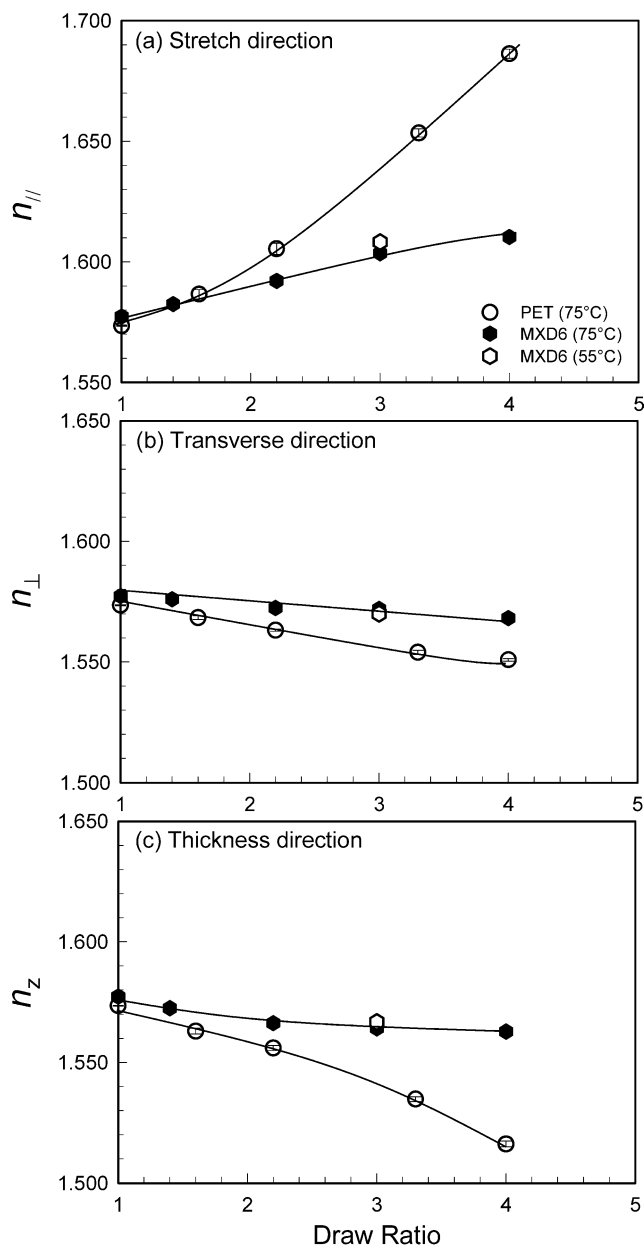


Fig. 1. Refractive index of PET and MXD6 as a function of constrained uniaxial draw ratio: (a) stretch; (b) transverse; and (c) thickness directions.

After drawing, the films were rapidly cooled to ambient temperature. The film thickness was about 0.10 mm after uniaxial stretching and about 0.09 mm after biaxial stretching.

The 12-oz and 2-l carbonated soft drink bottles made from PET and PET blends were supplied by INVISTA. The bottles were blown from pre-forms using a commercial blow-molding machine (Sidel). The bottle performs were stored at ambient condition overnight before blowing. The side wall temperature was nominally 90 °C. The blowing cycle time was 3 s. The wall section was cut from the bottle for subsequent characterization.

Refractive indices of the polyamide films were measured

with the Metricon 2010 prism coupler at 23 °C and 43% RH using a light source having a wavelength of 632.8 nm. Percent light transmittance was measured in accordance with ASTM D1746 using an UV-vis spectrometer at 630 nm wavelength. The film thickness for transparency measurements was 0.20, 0.10, and 0.09 mm for unoriented, uniaxially oriented and biaxially oriented films, respectively.

Oxygen flux at 43% relative humidity, 1 atm pressure, and 23 °C was measured with a MOCON OX-TRAN 2/20. Specimens were carefully conditioned as described previously [10]. Diffusivity D and permeability P were obtained by fitting the non-steady state flux-time curve to the solution to Fick's second law with appropriate boundary conditions [10]. Solubility S was calculated as $S = PD^{-1}$. Most of the specimens were tested within 1–3 days of stretching.

3. Results and discussion

3.1. Blends of PET with MXD6

The MXD6 refractive index (RI) of 1.5773 closely matched the PET refractive index of 1.5735. As a consequence of the close RI match, the light transmission (T) of compatibilized blends was almost as high as that of PET, 90% compared to 92%. One might have expected the blends to remain transparent, or even become more transparent, as they became thinner with stretching. However, stretching a blend with 10 wt% MXD6 to a draw ratio of 4 decreased T from 90 to 66%, whereas stretching PET decreased T only from 92 to 89%. Light transmission measured with unpolarized light is the average of the transmission in the directions parallel and perpendicular to stretching as measured with polarized light. The loss of transparency in the stretched blend was predominantly due to loss in the parallel direction, 46% compared to 81% in the perpendicular direction. Biaxial stretching (2.7×2.7) similarly reduced the transparency of the blend from 90 to 70%, compared to the change from 92 to 89% for PET.

Uniaxial stretching transforms spherical MXD6 particles into elongated ellipsoids, and biaxial stretching further deforms them into flat platelets [2]. Although the particle size in the film plane increases significantly as a result, particle size should not have such a profound effect on transparency if the refractive index match is maintained. The effect of stretching on the refractive index of PET and MXD6 is compared in Fig. 1. Uniaxial stretching increased the refractive index in the stretch direction (n_{\parallel}) and decreased the refractive index in the transverse (n_{\perp}) and thickness (n_z) directions. However, the effect of draw ratio on refractive index was much larger for PET than for MXD6. As a consequence, the refractive index difference particularly in the stretch direction became larger as the

Table 1
Refractive index of stretched PET and MXD6

Material	Unstretched	Uniaxially stretched ^a		Biaxially stretched ^b	
	n	n_{\parallel}	n_{\perp}	$n_{\parallel,1}^c$	$n_{\parallel,2}^d$
PET	1.5735	1.6863	1.5529	1.5984	1.6360
MXD6	1.5773	1.6103	1.5682	1.5854	1.5913
$ n_{\text{PET}} - n_{\text{MXD6}} $	0.0038	0.0760	0.0153	0.0130	0.0447

^a Draw ratio 4.0.

^b Draw ratio 2.7×2.7 for PET and 2.7×2.4 for MXD6.

^c Parallel to first stretch.

^d Parallel to second stretch.

draw ratio increased. For example, stretching PET at 75 °C to draw ratio of 4.0 increased the refractive index mismatch from 0.0038 before stretching to 0.0760 in the stretch direction and to 0.0153 in the transverse direction, Table 1. The dramatic increase in n_{\parallel} mismatch accounted for the loss of transparency in the stretch direction. Biaxial orientation only slightly reduced the refractive index mismatch to 0.0130 parallel to the first stretch and to 0.0447 parallel to the second stretch. Decreasing the draw temperature of MXD6 from 75 °C (above T_g at 43% RH) to 55 °C (below T_g) did not affect the relationship between RI and draw ratio.

3.2. Refractive index of stretched PET and MXD6

The relationship between optical anisotropy or birefringence and molecular orientation is described as

$$\Delta n = \Delta n_0 \langle P_2 \rangle \quad (1)$$

where Δn is the observed birefringence defined as the refractive index difference between stretch and thickness directions ($n_{\parallel} - n_{\perp}$), Δn_0 is the intrinsic birefringence, defined as Δn for perfect orientation, and $\langle P_2 \rangle$ is the orientation parameter or Hermans function [11]. Chemical structure determines Δn_0 ; it can be obtained experimentally

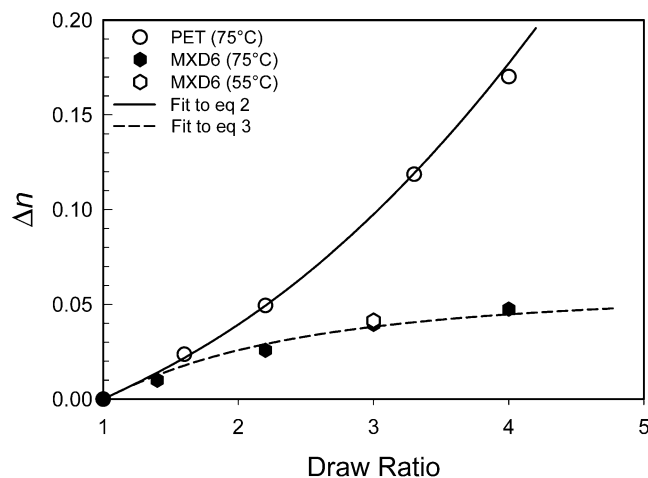


Fig. 2. Birefringence of PET and MXD6 as a function of constrained uniaxial draw ratio.

by extrapolation or estimated by additivity of bond polarizabilities.

Two theoretical approaches for predicting Δn_0 have been proposed: the affine and pseudo-affine deformation models [11–13]. In the affine model, network junctions are thought to be connected by flexible chains. Upon stretching, the network points are displaced in direct proportion to the macroscopic deformation. Consequently, the rotatable ‘random links’ comprising the network chains gradually adopt a more and more oriented configuration. For this type of rubber-like deformation, the orientation parameter ($\langle P_2 \rangle$) can be described as

$$\langle P_2 \rangle = \frac{\Delta n}{\Delta n_0} = \frac{1}{5N} \left(\lambda^2 - \frac{1}{\lambda} \right) \quad (2)$$

where N is the number of random links between network points and λ the draw ratio.

In pseudo-affine deformation, on the other hand, the structural elements undergoing deformation are assumed to have no extensibility themselves, but are rigid entities that simply rotate in proportion to the macroscopic deformation. The resulting expression for the orientation parameter is

$$\langle P_2 \rangle = \frac{\Delta n}{\Delta n_0} = \frac{1}{2} \left(\frac{2\lambda^3 + 1}{\lambda^3 - 1} - \frac{3\lambda^3}{(\lambda^3 - 1)^{3/2}} \arctan(\lambda^3 - 1)^{1/2} \right) \quad (3)$$

The birefringence of PET stretched at 75 °C and MXD6 stretched at two temperatures is shown as a function of draw ratio in Fig. 2. The slightly concave shape of the PET curve suggests that orientation of PET films follows the affine deformation model. This result is consistent with various studies of melt-spun PET fibers and of PET drawn above the T_g [14–16]. The solid line represents the fit of Eq. (2) with N of 4, which gives Δn_0 of 0.224 in good agreement with literature values of 0.21–0.24 for amorphous and crystalline PET [17,18]. The convex shape of the MXD6 curve indicates that orientation of MXD6 follows the pseudo-affine model. The experimental data are satisfactorily described by Eq. (3) with Δn_0 of 0.060 independent of stretching temperature. Reportedly, nylon6 fibers also follow the pseudo-affine model irrespective of spinning

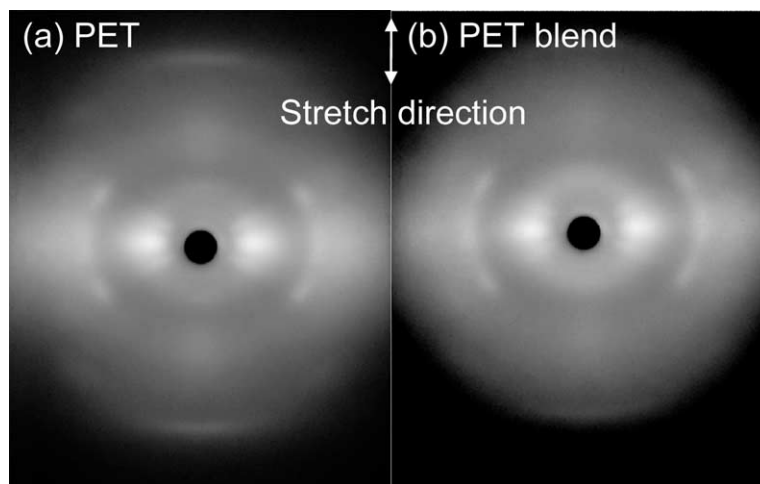


Fig. 3. Wide angle X-ray patterns after constrained uniaxial stretching to target draw ratio of 4: (a) PET; and (b) compatibilized PET blend with 10 wt% MXD6.

temperature and rate [12]. It may be that this is a general characteristic of polyamides caused by the hydrogen bonding network.

Large Δn_0 of PET in the parallel direction is attributed to the high degree of molecular orientation that can be achieved with the linear configuration of the backbone aromatic rings. The tendency for PET chains to align during stretching, which produces large Δn_0 , also gives rise to strain-induced crystallization, Fig. 3. The blend similarly undergoes strain-induced crystallization, which suggests that the MXD6 phase does not inhibit chain orientation of the PET matrix. On the other hand, meta-substitution on the aromatic ring of MXD6 hinders molecular alignment leading to Δn_0 for MXD6 which is even lower than Δn_0 for nylon6 of 0.067–0.089 [19]. One approach to increasing transparency of oriented blends aims at reducing Δn_0 of PET, and thereby achieving a closer RI match between the stretched matrix and stretched MXD6. Partial replacement of terephthalate with meta-substituted isophthalate should disrupt molecular alignment and thereby reduce the polarizability in the stretch direction.

3.3. Copolyesters containing isophthalate

Up to 30% of the terephthalate in PET was replaced with

isophthalate either by conventional copolymerization or by melt blending PET with poly(ethylene isophthalate) (PEI). Conventional copolymerization produced statistical copolymers, whereas some level of transesterification during melt processing of PET/PEI dry blends resulted in blocky copolymers [8]. The thermal properties of statistical and blocky copolymers are compared in Table 2. All the copolymers exhibited a single glass transition at a temperature intermediate between the glass transition temperatures of PET and PEI. Statistical incorporation of isophthalate effectively retarded cold-crystallization from the glass. At a heating rate of $10\text{ }^\circ\text{C min}^{-1}$, PET-co-20I exhibited only a small amount of cold-crystallization, as indicated by ΔH_{cc} , and PET-co-30I exhibited no detectable cold-crystallization. In contrast, blocky copolymers with up to 30% isophthalate readily cold-crystallized to high levels of crystallinity. The thermal properties were consistent with previous results for copolymers of well-characterized blockiness that were also obtained by melt blending PET and PEI [8].

The refractive index of unoriented PET and PEI was the same. As a consequence, all the copolymers had RI of 1.5735. The effect of stretching is shown in Fig. 4 with n_{\parallel} , which experienced larger changes than n_{\perp} and n_z . There was almost no change in RI of PEI as it was stretched to

Table 2
Properties of PET, PEI and copolymers

Material	IV (dL g ⁻¹)	T_g (°C)	T_{cc} (°C)	ΔH_{cc} (J g ⁻¹)	T_m (°C)	ΔH_m (J g ⁻¹)	Δn_0
PET	0.84	78	139	35	247	41	0.224
PET-co-7I	0.84	77	147	29	231	34	0.170
PET-co-20I	0.58	68	171	1.2	205	1.4	0.080
PET-co-30I	0.53	66	–	0	–	0	0.025
PET-b-15I	–	74	141	29	241	37	0.140
PET-b-20I	–	73	140	31	240	37	0.115
PET-b-25I	–	72	141	29	239	35	0.115
PET-b-30I	–	70	143	27	230	30	0.090
PEI	0.76	61	–	0	–	0	–

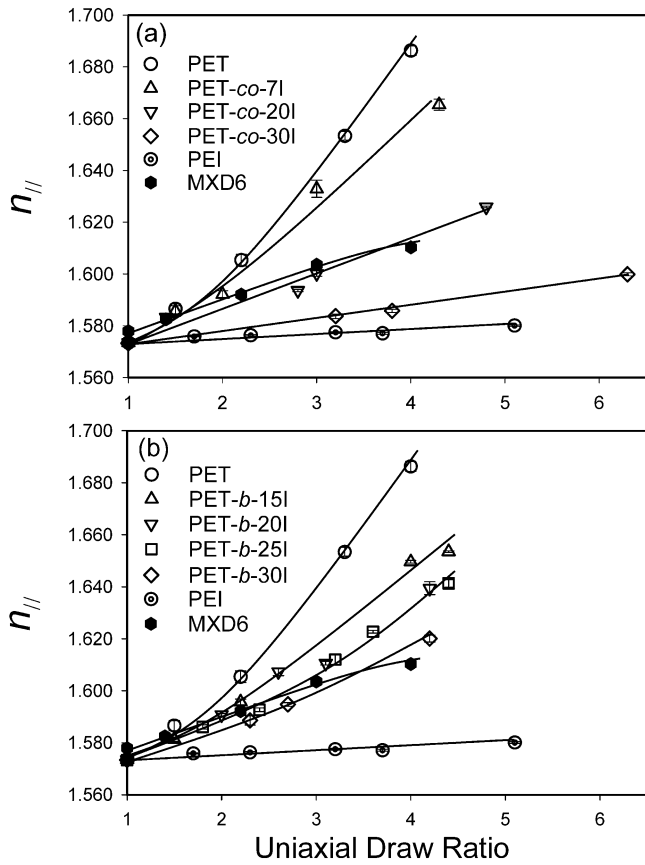


Fig. 4. Refractive index of PET, PEI, copolymers, and MXD6 as a function of uniaxial draw ratio: (a) statistical copolymers; and (b) blocky copolymers.

draw ratio of 5. The copolymers were intermediate between PET and PEI. For any draw ratio, $n_{||}$ decreased with increasing isophthalate content, and n_{\perp} and n_z (not shown) increased. The slightly concave shape of the $n_{||}$ curves indicated that orientation of the copolymers followed the affine deformation model with gradually decreasing Δn_0 . Values of Δn_0 from Eq. (2) with N of 4 are included in Table 2. Among the statistical copolymers, the reduction in $n_{||}$ achieved with PET-co-20I produced a good match with MXD6, Fig. 4(a). Among the blocky copolymers, a good match was achieved with PET-b-20I and PET-b-25I for draw ratio up to 3, Fig. 4(b). For higher draw ratio, the match was better with PET-b-30I. In general, $n_{||}$ and Δn_0 , Table 2, were higher for a blocky copolymer than for a statistical copolymer of the same composition. This result was consistent with a previous observation that blocky copolymers develop molecular orientation more readily than statistical copolymers [8].

3.4. Blends of copolyesters with MXD6

The morphology of compatibilized blends with 10 wt% MXD6 is shown in Fig. 5. In most of the blends, compatibilization resulted in good dispersion of spherical

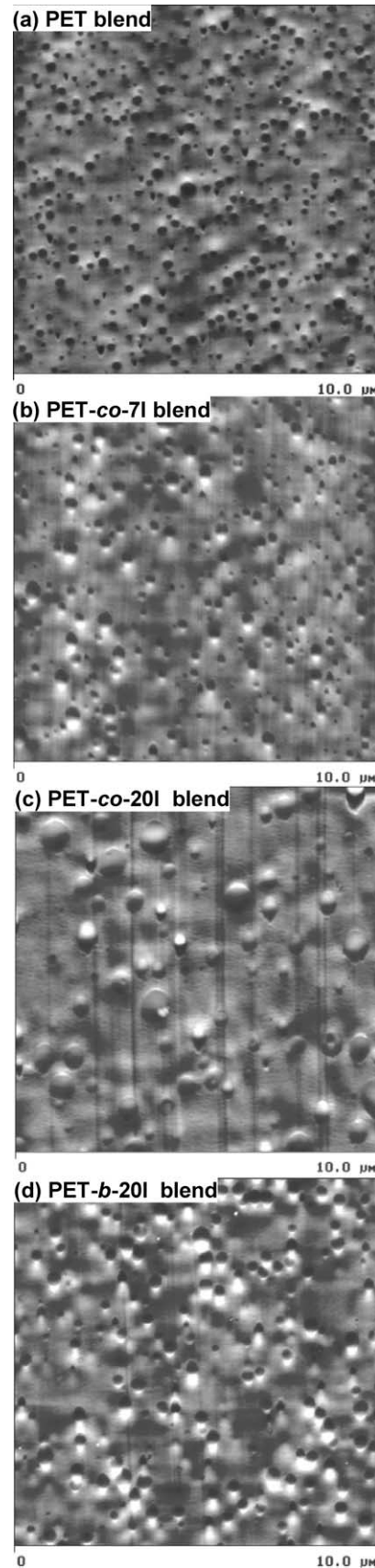


Fig. 5. AFM height images of compatibilized blends with 10 wt% MXD6 before stretching: (a) PET blend; (b) PET-co-7I blend; (c) PET-co-20I blend; and (d) PET-b-20I blend.

MXD6 particles about 0.3 μm in diameter. However, the particle size was as high as 0.9 μm in PET-co-20I and PET-co-30I blends, which was probably due to the low molecular weight and resulting low viscosity of PET-co-20I and PET-co-30I.

Thermograms of all the dry blends exhibited an inflection at about 75 $^{\circ}\text{C}$ corresponding to T_g of the matrix and a much weaker inflection at about 85 $^{\circ}\text{C}$ corresponding to T_g of MXD6. Like PET, all the blocky copolymers cold-crystallized readily in blends to achieve a high level of crystallinity, Table 3. The MXD6 particles are known to have a nucleating effect on cold-crystallization of PET [1,2], as was seen with PET and the blocky copolymers as a slight decrease in T_{cc} . The nucleating effect was most noticeable with the statistical copolymers and became more dramatic as the isophthalate content increased, Fig. 6. Thus, for PET-co-7I, the nucleating effect of MXD6 was indicated by a decrease in T_{cc} . However, PET-co-20I, which almost did not cold-crystallize at a heating rate of 10 $^{\circ}\text{C min}^{-1}$, in the blend achieved the same level of cold-crystallization as the blocky copolymer. Even PET-co-30I demonstrated a significant level of cold-crystallization in the blend. This result was consistent with a previous finding that statistical copolymers can develop significant levels of crystallinity although crystallization is very slow [20].

Before stretching, all the blends showed good transparency of 90%, Table 4. After uniaxial stretching, transparency improved from 66% for the PET blend to 74% for the PET-co-7I blend. Polarized light showed that transparency in the stretch direction improved the most from 46 to 61%. Similarly, after biaxial stretching, transparency improved from 70% for the PET blend to 81% for the PET-co-7I blend.

Although PET-co-20I should have given an even better RI match according to Fig. 4(a), blends with this matrix were not pursued because of the low matrix molecular weight, the large MXD6 particle size, and the greater difficulty in stretching statistical copolymers compared to blocky copolymers [8]. Rather, blends were prepared with blocky copolymers having 15–30% isophthalate. After uniaxial stretching, all the blocky copolymer blends had higher transparency than the PET blend, Table 4. The biaxially stretched blends were even more transparent,

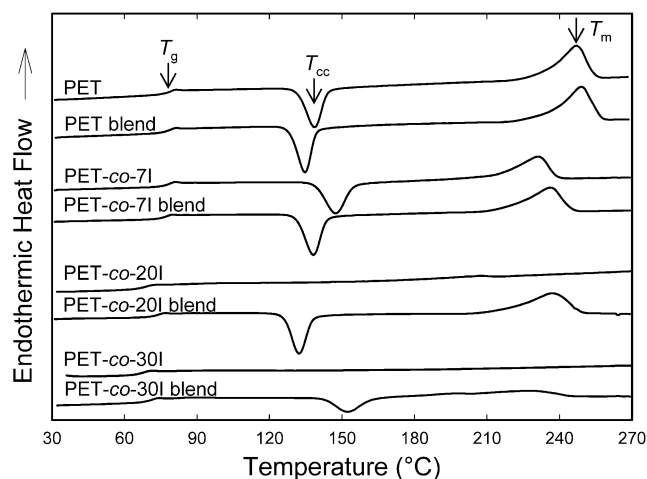


Fig. 6. Heating thermograms of dry polymers and compatibilized blends with 10 wt% MXD6.

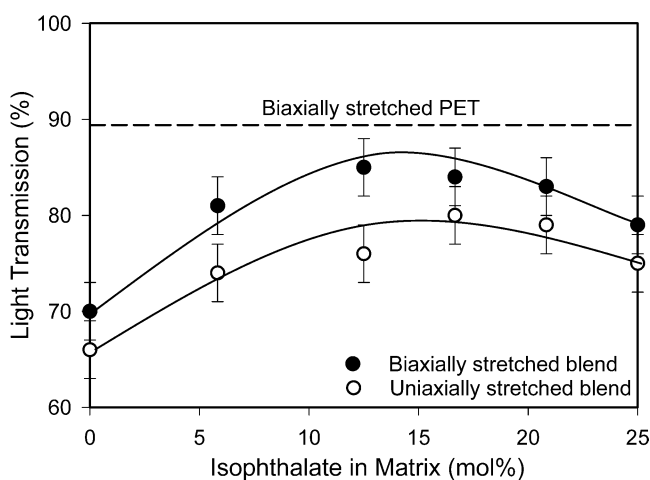


Fig. 7. Transparency of stretched blends with 10 wt% MXD6 as a function of matrix isophthalate content.

achieving 85% transmission, which was very close to the 89% transmission of biaxially stretched PET.

Transparency of uniaxially and biaxially stretched blends is plotted as a function of matrix isophthalate content in Fig. 7. Isophthalate in the blend matrix was somewhat lower than in the copolymer due to dilution from the compatibilizer. The plot shows a broad maximum with the highest

Table 3
Thermal analysis of dried blends with 10 wt% MXD6

Material	T_g ($^{\circ}\text{C}$)	T_{cc} ($^{\circ}\text{C}$)	ΔH_{cc} (J g^{-1})	T_m ($^{\circ}\text{C}$)	ΔH_m (J g^{-1})
PET	78	139	35	247	41
PET blend	78	133	32	248	39
PET-co-7I blend	77, 84	138	31	236	35
PET-co-20I blend	73, 85	132	28	237	36
PET-co-30I blend	70, 82	152	14	229	19
PET-b-15I blend	75, 85	136	29	243	37
PET-b-20I blend	73, 85	137	29	237	34
PET-b-25I blend	73, 85	138	27	234	30
PET-b-30I blend	72, 85	142	26	232	27

Table 4
Transparency of stretched blends

Material	Isophthalate content in matrix (mol%)	Unstretched ^a		Uniaxially stretched ^b		Biaxially stretched ^c		
		Unpolarized light <i>T</i> (%)	Unpolarized light <i>T</i> (%)	Polarized light		Unpolarized light <i>T</i> (%)	Polarized light	
				<i>T</i> (%)	<i>T</i> _⊥ (%)		<i>T</i> _{,1} ^d (%)	<i>T</i> _{,2} ^e (%)
PET	0	92	89	89	88	89	91	88
PET blend	0	90	66	46	81	70	72	66
PET- <i>co</i> -7I blend	6	90	74	61	84	81	–	–
PET- <i>b</i> -15I blend	13	90	76	71	84	85	84	84
PET- <i>b</i> -20I blend	17	90	80	77	85	84	84	85
PET- <i>b</i> -25I blend	21	90	79	73	84	83	82	82
PET- <i>b</i> -30I blend	25	90	75	70	79	79	78	78

^a Film thickness 0.20 mm.

^b Film thickness 0.10 mm, target draw ratio 4.

^c Film thickness 0.09 mm, target draw ratio 2.7×2.7.

^d Parallel to first stretch.

^e Parallel to second stretch.

transparency at a matrix isophthalate content of about 15%, which is somewhat lower than predicted from copolymer $n_{||}$ (Fig. 4). Possibly MXD6 particles hinder orientation of the blocky copolymer during stretching, which results in lower matrix $n_{||}$. Alternatively, blending with MXD6 exposes the copolymer to additional time in the melt, which increases the opportunity for further transesterification. Increased randomness would also hinder orientation leading to lower $n_{||}$.

Incorporation of isophthalate into PET has the additional advantage that it reduces the intrinsic gas permeability [9]. Permeability is reported to decrease from 0.424 for PET to 0.371 for PET-*b*-10I and further to 0.278 cm³(STP) cm m⁻² atm⁻¹ day⁻¹ for PET-*b*-20I [8]. However, orientation largely removes the effect of isophthalate on oxygen permeability, and lower intrinsic permeability of copolymers is offset by a smaller change in permeability after stretching [8]. Nevertheless biaxially stretched PET-*b*-15I maintains somewhat lower oxygen permeability than PET when tested at 43% RH, Table 5. However, the advantage does not carry over to the blend. The biaxially stretched PET blend and PET-*b*-15I blend have the same oxygen permeability. Very possibly, the strong tendency of PET chains to align, which produces high Δn_0 , is also responsible for the large reduction in oxygen permeability when PET is stretched. It follows that when isophthalate is incorporated to hinder chain alignment, and

thereby reduce Δn_0 , then stretching also becomes less effective in reducing oxygen permeability.

To the best of our knowledge, this is the first study in which good transparency was achieved in stretched PET blends by matching the refractive index of the constituents. The concept was validated for stretch-blown bottles. Results for 12-oz bottles showed that blending with 5 wt% MXD6 reduced transparency of the PET bottle wall from 93 to 78%, Table 6. However, replacing PET with PET-*co*-7I in the compatibilized blend improved transparency to 87%. Similar encouraging results were obtained with a blocky copolymer. Blending with 5 wt% MXD6 reduced transparency of 2-l PET bottle walls from 89 to 78%, whereas blending reduced the transparency of PET-*b*-20I bottle walls from 90 to 85% only.

4. Conclusions

Blends of PET with the aromatic polyamide MXD6 exhibit high gas barrier after biaxial orientation transforms the spherical polyamide particles into platelets of high aspect ratio. However, many packaging applications also require good transparency. Compatibilized blends of PET with MXD6 have good transparency in the unoriented glass because their refractive indices match closely. Unfortunately, haziness is observed after biaxial stretching because stretching imparts greater refractive index anisotropy to PET than to MXD6. Analysis of the strain-dependent birefringence reveals that different molecular deformation models describe the intrinsic birefringence of PET and MXD6. Hydrogen bonding of the polyamide may be responsible for the difference. Understanding the origin of blend haze leads to an approach for improving transparency of stretched PET blends. Replacing some of the terephthalate in PET with isophthalate decreases the glass transition temperature without affecting the refractive index. In

Table 5
Oxygen transport parameters after biaxial stretching tested at 43% RH

Material	<i>P</i>	<i>D</i>	<i>S</i>
PET	0.253	4.3	0.069
PET- <i>b</i> -15I	0.206	3.3	0.072
PET blend ^a	0.078	1.5	0.060
PET- <i>b</i> -15I blend ^a	0.078	1.7	0.054

^a Compatibilized blend with 10 wt% MXD6; *P*, [cm³(STP) cm m⁻² atm⁻¹ day⁻¹]; *D*, [×10⁻¹³ m² s⁻¹]; *S*, [cm³(STP) cm⁻³ atm⁻¹].

Table 6
Transparency of bottle walls

Material	Bottle size	Thickness (mm)	<i>T</i> (%)
PET	12-oz	0.24	93
PET blend ^a	12-oz	0.28	78
PET- <i>co</i> -7I blend ^a	12-oz	0.24	87
PET	2-1	0.32	89
PET- <i>b</i> -20I	2-1	0.26	90
PET blend ^a	2-1	0.28	78
PET- <i>b</i> -20I blend ^a	2-1	0.26	85

^a Compatibilized blend with 5 wt% MXD6.

addition, this study demonstrates that copolymerization with isophthalate reduces the intrinsic birefringence. Good refractive index match with stretched MXD6 requires copolymers with 15–20% isophthalate. Statistical copolymers in this composition range are not satisfactory for blending because of their low molecular weight and resistance to stretching. Alternatively, blocky copolymers of higher molecular weight are obtained by transesterification during melt blending of PET and PEI. Blocky copolymers with up to 30% isophthalate stretch readily at temperatures close to the T_g . After biaxial stretching, transparency of a copolymer blend with 10 wt% MXD6 approaches that of biaxially stretched PET. Improved transparency of copolymer blends compared to PET blends is validated with stretch-blown bottle walls.

Acknowledgements

The generous financial and technical support of INVISTA is gratefully acknowledged.

References

- [1] Prattipati V, Hu YS, Bandi S, Schiraldi DA, Hiltner A, Baer E, et al. *J Appl Polym Sci*. In press.
- [2] Hu YS, Prattipati V, Mehta S, Schiraldi DA, Hiltner A, Baer E. *Polymer* 2005;46:2685–98.
- [3] Watanabe T. *J Plast Film Sheeting* 1987;3:215–34.
- [4] Turner SR, Connell GW, Stafford SL, Hewa JD. US6444283; 2002.
- [5] Igarashi R, Watanabe Y, Hirata S. US4837115; 1989.
- [6] Maruhashi Y, Iida S. *Polym Eng Sci* 2001;41:1987–95.
- [7] Prattipati V, Hu YS, Bandi S, Mehta S, Schiraldi DA, Hiltner A, et al. *J Appl Polym Sci*. In press.
- [8] Liu RYF, Hu YS, Hibbs MR, Collard DM, Schiraldi DA, Hiltner A, et al. *J Appl Polym Sci*. In press.
- [9] Polyakova A, Liu RYF, Schiraldi DA, Hiltner A, Baer E. *J Polym Sci Part B: Polym Phys* 2001;39:1889–99.
- [10] Sekelik DJ, Stepanov EV, Nazarenko S, Schiraldi D, Hiltner A, Baer E. *J Polym Sci Part B: Polym Phys* 1999;37:847–57.
- [11] Ward IM, editor. *Structure and properties of oriented polymers*. London: Chapman & Hall; 1997. p. 1–43 [Chapter 1].
- [12] Penning JP, van Ruiten J, Brouwer R, Gabriëlse W. *Polymer* 2003;44:5869–76.
- [13] Hamza AA, Sokkar TZN, El-Farahaty KA, El-Dessouky HM. *Polym Test* 2004;23:203–8.
- [14] Nobbs JH, Bower DI, Ward IM. *J Polym Sci Polym Phys Ed* 1979;17:259–72.
- [15] Rietsch F, Duckett RA, Ward IM. *Polymer* 1979;20:1133–42.
- [16] Ward IM, Bleackley M, Taylor DJR, Cail JI, Stepto RFT. *Polym Eng Sci* 1999;39:2335–48.
- [17] Garg SK. *J Appl Polym Sci* 1982;27:2857–67.
- [18] Huijts RA, Peters SM. *Polymer* 1994;35:3119–21.
- [19] Balcerzyk E, Kozłowski W, Wesolowska E, Lewaszkiewicz W. *J Appl Polym Sci* 1981;26:2573–80.
- [20] Hu YS, Hiltner A, Baer E. *J Appl Polym Sci*. In press.